Stoch Environ Res Risk Assess (2018) 32:1771–1782
https://doi.org/10.1007/s00477-017-1471-3

ORIGINAL PAPER

A heuristic probabilistic approach to estimating size-dependent mobility of nonuniform sediment

Befekadu Taddesse Woldegiorgis[1] · Fu-Chun Wu[2] · Ann Van Griensven[1,3] · Willy Bauwens[1]

Published online: 2 November 2017

Abstract This paper presents a heuristic probabilistic approach to estimating the size-dependent mobilities of nonuniform sediment based on the pre- and post-entrainment particle size distributions (PSDs), assuming that the PSDs are lognormally distributed. The approach fits a lognormal probability density function to the pre-entrainment PSD of bed sediment and uses the threshold particle size of incipient motion and the concept of sediment mixture to estimate the PSDs of the entrained sediment and post-entrainment bed sediment. The new approach is simple in physical sense and significantly reduces the complexity and computation time and resource required by detailed sediment mobility models. It is calibrated and validated with laboratory and field data by comparing to the size-dependent mobilities predicted with the existing empirical lognormal cumulative distribution function approach. The novel features of the current approach are: (1) separating the entrained and non-entrained sediments by a threshold particle size, which is a modified critical particle size of incipient motion by accounting for the mixed-size effects, and (2) using the mixture-based pre- and post-entrainment PSDs to provide a continuous estimate of the size-dependent sediment mobility.

Keywords Nonuniform sediment · Particle size distribution · Mobility · Entrainment · Incipient motion

1 Introduction

The simulation of sediment size distribution in rivers is an important factor when studying sediment mobility, providing useful information for many sediment-related water problems, such as settling processes in reservoirs or the mobility of sediment-bound pollutants (Wu and Wang 1998). The study of partial transport is essential for understanding the size-selective processes of nonuniform sediment (Wu and Yang 2004a). Detailed sediment transport models split the particle size distribution into several size classes and evaluate the mobility of each size class by accounting for the variability of the near-bed hydrodynamic forces and the relative sheltering and exposure of mixed-size sediment particles (Wu and Yang 2004b). More detailed sediment models (Oh and Tsai 2017) account for a stochastic multivariate particle tracking that would take into consideration the randomness of both fluid and sediment particle trajectories. Such approaches are physically robust and provide reliable predictions of sediment mobility, yet are computationally demanding (Buscombe and Conley 2012).

The objective of this work is to develop a simple and computationally efficient, heuristic conceptual approach to estimating the size-dependent mobility of nonuniform sediments. The heuristic approach estimates the sediment mobility based on the pre- and post-entrainment particle size distributions (PSDs), assuming that the PSDs are

Electronic supplementary material The online version of this article (https://doi.org/10.1007/s00477-017-1471-3) contains supplementary material, which is available to authorized users.

✉ Befekadu Taddesse Woldegiorgis
befekadu.woldegiorgis@vub.be

[1] Department of Hydrology and Hydraulic Engineering, Vrije Universiteit Brussel (VUB), Pleinlaan 2, 1050 Brussels, Belgium

[2] Department of Bioenvironmental Systems Engineering, National Taiwan University, Taipei 106, Taiwan

[3] UNESCO-IHE Institute for Water Education, Delft, The Netherlands

lognormally distributed. The approach is simple in physical sense, yet interesting in methodological aspect. It fits a lognormal probability density function (PDF) to the pre-entrainment sediment PSD and uses the threshold grain size of incipient motion and the concept of sediment mixture to estimate the PSDs of the entrained and post-entrainment sediments. The approach is validated with laboratory and field data by comparing to the size-dependent mobilities predicted with the empirical lognormal cumulative distribution function (CDF) approach of Wu and Yang (2004b).

The remainder of this paper is structured as follows. Section 2 describes the conceptual framework and procedures of the heuristic PSD-based approach. Validation of the new approach with laboratory and field data is presented in Sect. 3. Concluding remarks are provided in Sect. 4.

2 Heuristic PSD-based approach for mobility estimation

Previous studies revealed that lognormal distributions are well suited for the PSDs of river sediments (Abuodha 2003; Bouchez et al. 2011; Agrawal et al. 2012), which is the assumption underpinning this approach. The lognormal assumption allows us to use many convenient properties of the normal distribution in the estimation of sediment mobility because the methodology for the mixture of two normals can be used by applying the natural logarithmic transformation to the lognormal distributions (Fowlkes 1979). The lognormal PDF used to express the PSD is given as follows:

$$P[\ln(d)|\mu,\sigma] = \frac{1}{\sigma\sqrt{2\pi}}\exp\left[-\frac{(\ln(d)-\mu)^2}{2\sigma^2}\right] \quad (1)$$

where d is the particle diameter, μ is the mean of the log-transformed particle diameters, and σ is the standard deviation of the log-transformed particle diameters.

2.1 Particle size distribution of sediment mixture

For two sediment samples with independent PSDs, their mixture PSD remains lognormally distributed (Eisenberg and Sullivan 2008). Although the sediment samples to be mixed in this study are correlated, their mixture can be approximated by a lognormal distribution because Safik and Safak (1994) have shown that the mixture of correlated lognormal distributions can be approximated as lognormal. The mean and standard deviation of the mixture PSD are determined by applying logarithmic transformations to the lognormal distributions and using the mixture of two normal distributions provided by Fowlkes (1979):

$$\mu_{mix} = P_a\mu_a + P_b\mu_b \quad (2)$$

$$\sigma^2_{mix} = P_a\sigma^2_a + P_b\sigma^2_b + P_aP_b(\mu_a-\mu_b)^2 \quad (3)$$

where μ_a and μ_b are the means of the sample PSDs; μ_{mix} is the mean of the mixture PSD; σ^2_a and σ^2_b are the variances of the sample PSDs; σ^2_{mix} is the variance of the mixture PSD; P_a and P_b are the mass fractions of the samples, and by definition $P_a + P_b = 1$. Here, samples a and b are taken to be the entrained and post-entrainment sediments, respectively, and mixture is taken to be the pre-entrainment sediment.

2.2 PSDs of entrained and post-entrainment sediments

Previous studies indicated that the incipient motion of mixed-size sediment is a complex process due to a number of factors associated with the hiding-exposure effect and bed armoring (Sundborg 1956; Wilcock and Southard 1988, 1989; Wu and Yang 2004a, b). Here we adopt an approach used by (Shrestha et al. 2013) that determines the entrained mass fraction based on the fraction of sediment finer than the critical particle size of incipient motion. This is done by calculating the area under the PSD curve to the left of the critical size d_{cr}, using the following lognormal CDF:

$$P_{ent} = P[d|d<d_{cr}] = \frac{1}{2}\mathrm{erfc}\left(-\frac{(\ln(d_{cr})-\mu)}{\sigma\sqrt{2}}\right) \quad (4)$$

where P_{ent} is the mass fraction of the bed sediment entrained. The mean and variance of the entrained sediment PSD, μ_{ent} and σ^2_{ent}, are determined using the truncation equations of the normal distribution (Rilstone 2002), given as follows:

$$\mu_{ent} = E[d|d<d_{cr}] = \mu - \sigma\left[\frac{\phi\left(\frac{\ln(d_{cr})-\mu}{\sigma}\right)}{\Phi\left(\frac{\ln(d_{cr})-\mu}{\sigma}\right)}\right] \quad (5)$$

$$\sigma^2_{ent} = Var[d|d<d_{cr}] = \sigma^2\left\{1-\left(\frac{\ln(d_{cr})-\mu}{\sigma}\right)\cdot\left[\frac{\phi\left(\frac{\ln(d_{cr})-\mu}{\sigma}\right)}{\Phi\left(\frac{\ln(d_{cr})-\mu}{\sigma}\right)}\right]-\left[\frac{\phi\left(\frac{\ln(d_{cr})-\mu}{\sigma}\right)}{\Phi\left(\frac{\ln(d_{cr})-\mu}{\sigma}\right)}\right]^2\right\} \quad (6)$$

where the operators ϕ and Φ are as defined as follows:

$$\phi\left(\frac{\ln(d_{cr})-\mu}{\sigma}\right) = \frac{1}{\sqrt{2\pi}}\exp\left[-\frac{(\ln(d_{cr})-\mu)^2}{2\sigma^2}\right] \quad (7)$$

$$\Phi\left(\frac{\ln(d_{cr})-\mu}{\sigma}\right)=\frac{1}{2}\left[1+\mathrm{erf}\left(\frac{\ln(d_{cr})-\mu}{\sigma\sqrt{2}}\right)\right] \quad (8)$$

The critical particle size of incipient motion d_{cr} is detrmined using an iterative procedure outlined as follows:

Step 1 An estimate of the critical particle size d_{cr} is specified.

Step 2 The critical particle size d_{cr} is converted into a dimensionless grain size D_* as follows:

$$D_*=d_{cr}\left[\frac{(s-1)g}{v^2}\right]^{1/3} \quad (9)$$

where s is specific gravity of sediment (= 2.65), g is gravitational acceleration, and v is kinematic viscosity of water.

Step 3 The dimensionless critical shear stress (critical Shields parameter) θ_{cr} corresponding to D_* is calculated using the following equation (Soulsby and Whitehouse 1997):

$$\theta_{cr}=0.22D_*^{-0.9}+0.055[1-\exp(-0.02D_*)] \quad (10)$$

Step 4 The critical bed shear stress τ_{cr} required to entrain the particle size d_{cr} is calculated using the relation between Shields parameter and bed shear stress:

$$\tau_{cr}=\theta_{cr}\gamma(s-1)d_{cr} \quad (10)$$

where γ is specific weight of water.

Step 5 The mean bed shear stress τ_0 is calculated as follows using the available flow variables:

$$\tau_0=\gamma RS \quad (11)$$

where R is hydraulic radius; S is bed slope. The mean bed shear stress τ_0 is corrected for the sidewall effect using the method of Vanoni and Brooks (1957).

Step 6 The critical bed shear stress τ_{cr} is compared to the mean bed shear stress τ_0, and the difference between the two is calculated. Steps 1–5 are repeated until the difference becomes negligible. For this, we used the "Goal seek" optimization tool available in the Excel spreadsheet. The objective function is the difference calculated in step 6 and the parameter to be changed is the critical particle size d_{cr} estimated in step 1. The "Goal seek" optimization tool keeps changing the estimated value of the critical particle size d_{cr} until the difference between the objective function values of two successive iterations becomes < 0.001.

It is noted here that the critical particle size d_{cr} so determined is for the bed composed of uniform sediment. This uniform-sediment-based critical particle size of incipient motion will be modified in Sect. 2.3 to take into account the mixed-size effect of nonuniform sediment.

Literature shows that the reach-average bed shear stress is not appropriate for determining the variability of local, small scale shear stress (Biron et al. 2004). The methods used to compute the shear stress of non-uniform flow require (Graf and Song 1995): (1) determination of the velocity profile or, (2) determination of Reynolds-stress profile or, (3) utilization of the dynamic St. Venant equations or, (4) direct measurement of the skin friction. These methods are rather detailed and require computationally expensive hydraulics calculations.

The whole idea of the new method is to provide a rapid assessment of sediment mobility. Although the mean bed shear stress is calculated with the assumption of uniform flow condition, it can be used to give a preliminary estimate of the sediment mobility under gradually varied flow conditions as it is usual to: (1) estimate the slope of the energy grade line of gradually-varied flows from uniform flow formulas with uniform flow resistance coefficients, and (2) use the local depth as though the flow were locally uniform (Schulte and Chaudhry 1987; Rhodes 1995). The fact that the shear velocity determined for accelerating and decelerating flows only slightly changes in the direction of flow when the rate of change of water depth is mild (in the range [− 0.01, 0.01]). Graf and Song (1995) showed that the influence of flow acceleration on the bed shear stress under this type of gradually varied flow is not significant. When the rate of change of water depth is mild, the effect of pressure gradient also becomes insignificant. The use of the mean bed shear stress that is calculated with the assumption of uniform flow condition has been successfully used to simulate sediment erosion for modelling transient bed profiles in alluvial channels (Tayfur and Singh 2007). Also, Wu et al. (2000) suggested the use of the mean bed shear stress that is calculated with the assumption of uniform flow condition for natural rivers, and they successfully used this assumption to simulate the fractional bed load transport of alluvial rivers. Consequently, the uniform-flow assumption can provide reasonable estimates of bed shear stress for gradually-varied flows in natural rivers.

Only the bed shear stress corresponding to the grain roughness should be used for bed load mobility when sand ripples and dunes exist on the bed (Wu et al. 2000). The experimental data do not have bed form resistance; hence no correction is needed to separate the skin friction from the total bed resistance except to correct for the effect of smooth wall. On the other hand, the field data were collected from a natural river that has sand dunes (Leopold and Emmettt 1976). In order to make explicit use of the bed stress caused by the grain resistance for the calculation of sediment mobility, we used the formula provided by Wu et al. (2000).

$$\tau_o' = \left(\frac{n'}{n}\right)^{3/2} \tau_o \tag{12}$$

where τ' is the grain shear stress, n is the Manning's roughness coefficient of the channel bed, and n' is the Manning's roughness coefficient corresponding to the grain roughness, calculated according to the suggestion of Church et al. (1990) and used by Wu and Wang (2000) and Wu et al. (2000).

$$n' = \frac{(d_{50})^{1/6}}{20} \tag{13}$$

where d_{50} is the median size of the sediment obtained from the field data

The Manning's roughness coefficient of the channel bed is determined by

$$n = \frac{R^{2/3} S_f^{0.5}}{U} \tag{14}$$

where R is the hydraulic radius (m), U is the mean flow velocity (ms^{-1}), and S_f (−) is the friction slope (−). All the three hydraulic variables are obtained from the field data, and the water surface slope is used to approximate the friction slope.

The Manning's roughness coefficient corresponding to the grain roughness (n') is expected to be lower than that of the channel bed (n). However, the computed results do not satisfy this condition because water surface slope is used to approximate friction slope. Nevertheless, an assumption could be taken that the grain resistance is dominant as compared to the bed form drag from this information. Consequently, the mean bed shear stress calculated using Eq. (11) is assumed to be equal to the grain shear stress.

We assume that the PSDs of the entrained sediment and post-entrainment bed sediment also follow lognormal distributions. The critical particle size of incipient motion is only used to estimate the mass fraction of the entrained sediment. Thus, abrupt truncation PDFs are used neither for the bed sediment nor for the entrained sediment. Entrainment is a continuous process, hence any PSD of bed sediment may be considered as a post-entrainment sample in reference to some time point before the sample was collected. The fact that lognormal distributions usually fit to the sediment PSDs (Abuodha 2003; Bouchez et al. 2011; Agrawal et al. 2012) implies that the bed sediment PSDs follow lognormal distributions both before and after the entrainment. Lognormal distributions fitted to the PSD data we obtained from literature (Leopold and Emmettt 1976; Wilcock and Mcardell 1997; Sun and Donahue 2000; Wu and Yang 2004a) further validate our assumption (see "Appendix 1").

The assumption of lognormal PSDs mimics the partial transport of sediment by avoiding the problem of abrupt truncations and thereby enabling the entrainment of fractions of some size ranges of the bed sediment PSD. A partial transport occurs when the mobility of at least one particle size is greater than zero (Wu and Yang 2004a). We will show in Sect. 3 how this approach mimics the size-dependent mobilities predicted with the existing empirical approach presented by Wu and Yang (2004b).

The mean and variance of the post-entrainment PSD, μ_{post} and σ^2_{post}, are evaluated using Eqs. (2) and (3), expressed as follows:

$$\mu_{post} = \left(\frac{1}{1-P_{ent}}\right)\mu_{pre} - \left(\frac{P_{ent}}{1-P_{ent}}\right)\mu_{ent} \tag{15}$$

$$\sigma^2_{post} = \left(\frac{1}{1-P_{ent}}\right)\sigma^2_{pre} - \left(\frac{P_{ent}}{1-P_{ent}}\right)\sigma^2_{ent} - P_{ent}(\mu_{ent} - \mu_{post})^2 \tag{16}$$

in which P_{ent}, μ_{ent}, and σ^2_{ent} are determined from Eqs. (4)–(6).

2.3 Threshold particle size for incipient motion of mixed-size sediment

In mixed-size sediment, particles of smaller sizes tend to hide among the coarser particles and hence the critical bed shear stress needed to entrain the smaller particles may be greater than that needed to entrain uniform sediment of the same size (Armanini and Di Silvio 1988; Wu and Yang 2004a). The uniform-sediment-based critical size of incipient motion, d_{cr}, determined through Eqs. (9)–(12) has to be modified. The modified threshold particle size of incipient motion, d_2, takes into account the hydraulic variables that influence the entrainment and an index that represents the nonuniformity of the sediment PSD, and is expressed as:

$$d_2 = d_{cr} \cdot \left(\frac{\alpha \cdot \mathrm{Re}}{CV \cdot D_*^{\beta}}\right) \tag{17}$$

where $\alpha = 1.44 \times 10^{-4}$ and $\beta = 0.286$ are coefficients calibrated by reproducing the size-dependent sediment mobilities predicted with the empirical lognormal CDF of Wu and Yang (2004b) using the PSDs and hydraulic conditions from a laboratory dataset (Wu and Yang 2004a) and a field dataset (Leopold and Emmettt 1976) (see Sect. 3.1 for details); $\mathrm{Re} = UD/\nu$ is Reynolds number, U and D are mean flow velocity and depth, ν is kinematic viscosity; CV is the coefficient of variation of the PSD, defined as the ratio of standard deviation to mean size (Jafari et al. 2011); D_* is dimensionless grain size defined in (9). Incorporation of CV in (15) is crucial, as it takes into account the variability of particle sizes and the resulting hiding-exposure effects on the entrainment of mixed-size sediment.

2.4 Size-dependent mobility of nonuniform sediment

For the lognormal PSD of the pre-entrainment bed sediment (PDF1), as illustrated in Fig. 1, the area integrated between any two particle sizes on the abscissa is the mass fraction of sediment within the given size range, given that the total area under the PSD curve is equal to 1. The PSD of the post-entrainment bed sediment (PDF2), determined using (13) and (14), will have a shift in the mean and standard deviation from the corresponding values of PDF1 but the same total area. The total mass of the post-entrainment bed sediment is less than the total mass of the pre-entrainment bed sediment. As both PSDs have the same area but represent different amounts of total mass, it is necessary to rescale the area under PDF2 by a factor of $1 - P_{ent}$. Here, the rescaled PDF2 is denoted as PDF2'. The ratio of the difference between PDF1 and PDF2' to PDF1 provides a continuous estimate of the size-dependent mobility Y of the bed sediment (Fig. 1), as expressed by:

$$Y = \frac{PDF1 - PDF2'}{PDF1} \tag{18}$$

By varying the threshold particle size of incipient motion over a range for different PSDs, we learned that PDF2' assumes values less than or equal to PDF1. In very few cases PDF2' is marginally greater than PDF1, e.g., the upper right flank of the PSDs shown in Fig. 1. In such cases, we eliminated the marginal differences so that the mass of bed sediment does not gain due to entrainment. The higher the applied bed shear stress (right panel, Fig. 1), the greater the threshold particle size and thus the mean size of the entrained sediment. This results in a shift to the right and a reduction of the ordinates of PDF2' and, consequently, an increase in the mobility of the coarser particles. This is in agreement with the published data (Wilcock and Mcardell 1997; Wu and Yang 2004a) and indicates that the working principle of this new approach is internally consistent. The new method provides a continuous estimate of the size-dependent sediment mobility and thereby allows some degree of mobility for sediment sizes that are coarser than d_2. This is in agreement with the conclusions of Lavelle and Mofjeld (1987) and Lopez and Garcia (2001) whereby they found that some sediment size fractions move at a time-mean bed stress lower than their corresponding critical stresses for incipient motion.

2.5 Calibration and validation

To calibrate and validate the proposed PSD-based approach for mobility estimation, we used four sets of published data, including three from laboratory experiments (Wilcock and Mcardell 1997; Sun and Donahue 2000; Wu and Yang 2004a) and one from a field study (Leopold and Emmettt 1976). The dataset of Wilcock and Mcardell (1997) included 5 runs with 5 PSDs; the dataset of Sun and Donahue (2000) included 9 runs with 4 PSDs; the dataset of Wu and Yang (2004b) included 7 runs with 1 PSD; the data of Leopold and Emmettt (1976) from the East Fork River (Wyoming, US) included 12 PSDs

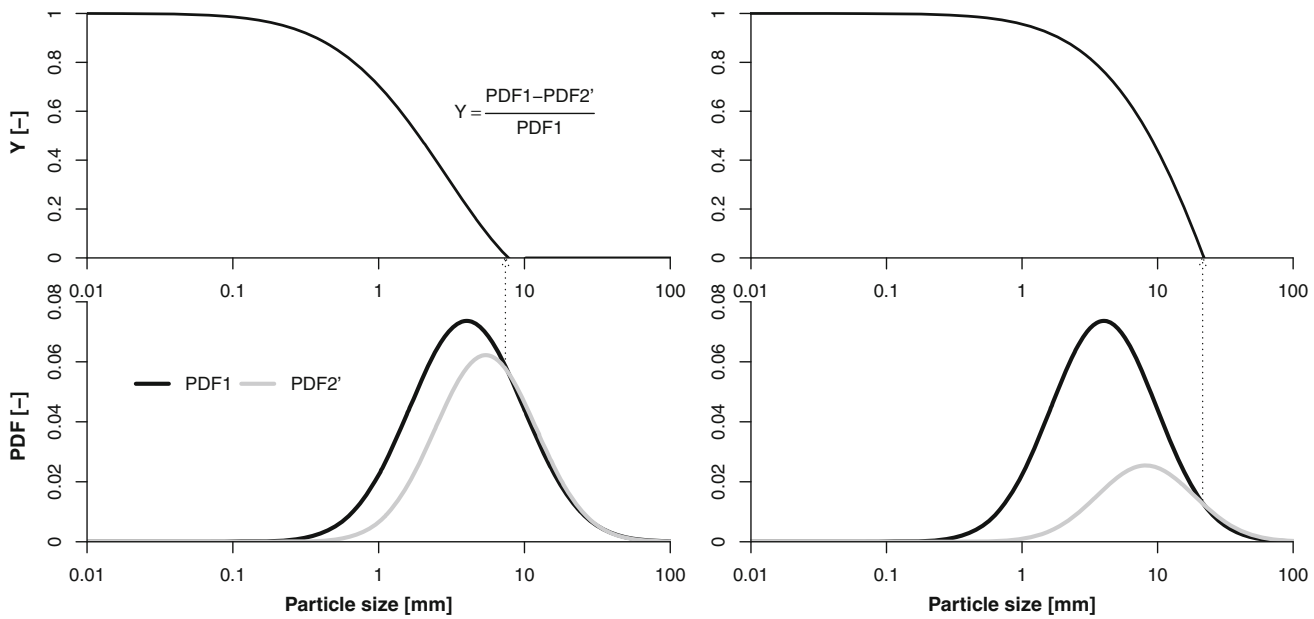

Fig. 1 Size-dependent mobility of the same sediment subjected to different bed shear stresses: left panel, lower shear stress; right panel, higher shear stress

collected in 1974. All these PSDs were fitted with the lognormal PDFs. The parameters (means and standard deviations) of the best-fit PSDs are summarized in "Appendix 1" (see Table 1), where the graphical comparisons of the measured and fitted CDFs of grain sizes are also shown. A compilation of the hydraulic conditions of the four datasets is provided in "Appendix 2" (see Tables 2, 3, 4, 5).

Among these four datasets, the laboratory data of Wu and Yang (2004b) and the field data of Leopold and Emmettt (1976) were used for calibration of the modified threshold particle size. Once calibrated, the new approach was validated with the other two sets of laboratory data (Wilcock and Mcardell 1997; Sun and Donahue 2000) and additional two sets of field data collected in 1973 and 1975 (Leopold and Emmettt 1976).

Calibration of the threshold grain size d_2 was performed by reproducing the size-dependent mobilities predicted with the empirical lognormal CDF of (Wu and Yang 2004a), where they fitted a lognormal CDF to the mean trend of the backcalculated size-dependent mobilities (using their stochastic partial transport model) as a function of the dimensionless effective shear stress θ'_d, which is defined by:

$$\theta'_d = \theta_d \left[\sigma_g^{0.25} \left(\frac{d}{d_m} \right)^{0.5} \right] \tag{19}$$

where $\theta_d = \tau_0/\gamma(s-1)d$ is the dimensionless shear stress (shields parameter) based on particle size d; σ_g is geometric standard deviation of the PSD; d_m is mean particle size. The term in the square bracket is a correction for the hiding-exposure effects on the shear stress applied on the mixed-size sediment. The mean and standard deviation of the empirical lognormal CDF, μ_{LN} and σ_{LN}, vary as a function of the sand content f_s, which are given as follows (Wu and Yang 2004a):

$$\begin{cases} \mu_{LN} = -0.058 f_s + 0.046 & \text{for} \quad f_s < 0.34 \\ \sigma_{LN} = -0.088 f_s + 0.017 & \text{for} \quad f_s < 0.34 \\ \mu_{LN} = 0.0263 & \text{for} \quad f_s \geq 0.34 \\ \sigma_{LN} = 0.0076 & \text{for} \quad f_s \geq 0.34 \end{cases} \tag{20}$$

The sand contents in the four sets of data are also summarized in "Appendix 2" (see Tables 2, 3, 4, 5). The size-dependent mobilities predicted with the empirical lognormal CDF of Wu and Yang (2004b) are used in this study as a reference for evaluating the performance of our approach. For convenience, hereinafter the empirical lognormal CDF of Wu and Yang (2004b) is referred to as 'CDF_Wu2004b'.

3 Results and discussion

3.1 Effect of modified threshold particle size

The improvement of the threshold particle size d_2 over the uniform-sediment-based critical size d_{cr} is shown here. The size-dependent mobilities estimated with the PSD-based approach using the uniform-sediment-based critical size d_{cr} along with the results predicted with the CDF_Wu2004b are shown in Fig. 2, with the PSDs and hydraulic conditions of the calibration datasets used as the inputs (Leopold and Emmettt 1976; Wu and Yang 2004a). As it is revealed, our estimated mobilities of the coarser particles (i.e., smaller dimensionless effective shear stresses) are significantly underestimated as compared to the results predicted with the CDF_Wu2004b. This is supported by the previous findings that without considering the exposure effect of the coarser particles the mobilities would be underestimated (Armanini and Di Silvio 1988; Wilcock and Mcardell 1997). This also highlights the need for a correction of the critical size d_{cr} that is determined for the incipient motion of uniform-size sediment where no mixed-size effects are present.

The correction factor for the threshold particle size d_2 given in (15) was calibrated by reproducing the size-dependent mobilities predicted with the CDF_Wu2004b. The results obtained with the PSD-based approach using the modified threshold size d_2 are shown in Fig. 3, along with the results predicted with the CDF_Wu2004b. For both data, the results obtained using the modified threshold particle size d_2 show satisfactory agreement with the results predicted with the CDF_Wu2004b. The statistical goodness-of-fit measure R^2 gives a value of 0.88 for the laboratory data and 0.95 for the field data. The mobilities of the coarser particles are much improved, while the mobilities of the finer particles (greater dimensionless effective shear stresses) are slightly underestimated for the laboratory data. Since emphasis is given here to capture the size-dependent pattern of sediment mobility rather than to achieve a high goodness-of-fit measure, exact reproduction of the mobilities predicted with the CDF_Wu2004b is deemed not necessary though partly because CDF_Wu2004b is a lognormal fit to the mean trend of the backcalculated size-dependent mobilities for each of the datasets used.

3.2 Validation with laboratory and field data

The calibrated PSD-based approach was further validated with two other laboratory data (Wilcock and Mcardell 1997; Sun and Donahue 2000) and two additional field datasets collected in 1973 and 1975 (Leopold and Emmettt

1976), the results are shown in Figs. 4 and 5, respectively. Overall, for these four validation datasets, the size-dependent mobilities estimated with the PSD-based approach follow satisfactorily the trends predicted with the CDF_Wu2004b. The PSD-based approach underestimates the mobilities of the laboratory data of Wilcock and Mcardell (1997) for dimensionless shear stresses between 0.03 and 0.09 (Fig. 4, left panel). These underestimated mobilities correspond to the runs with smaller bed shear stresses where the mobilities are sensitive to the variability in bed shear stress, which is in agreement with the findings of Wilcock and Mcardell (1997). The underestimations of the mobilities at dimensionless effective shear stress greater than 0.09, however, cannot be attributed to the variability in bed shear stress; they are attributed to the limitation of the PSD-based approach. The mobility of the fine sediments simulated by the PSD-based approach is sensitive to the changes in the tail part of the PDF fitted to the PSD. Generally, the PSD-based approach predicts underestimated mobilities of fine sediments for high bed shear stresses combined with small ratios of d_2 to d_{cr}. On the other hand, the mobilities estimated with the PSD-based approach for the laboratory data of Sun and Donahue (2000) well capture the pattern of the mobilities predicted with the CDF_Wu2004b (Fig. 4, right panel). The scatter of the PSD-based mobilities reflects the variability of the incipient motion with the effective bed shear stress. Such scatter is not abnormal given that the CDF_Wu2004b is a lognormal fit to the mean trend of the backcalculated size-dependent mobilities for each of the datasets used.

The size-dependent mobilities estimated with the PSD-based approach generally agree with the results predicted with the CDF_Wu2004b for the 1973 data of East Fork River (Fig. 5, left panel), while the mobilities estimated with the PSD-based approach for the 1975 data of East Fork River (Fig. 5, right panel) show a wider scatter. Given that the variability in the bed shear stresses of the 1975 data is high, the scatter of the mobilities estimated with the PSD-based approach is natural according to the findings of Wilcock and Mcardell (1997). The data points with small flow velocities have small Reynolds numbers and small bed shear stresses that result in small critical particle sizes estimated for uniform sediments (d_{cr}). Consequently, Eq. (15) yields small values of d_2. The smaller the d_2, the smaller is the entrained mass and hence the smaller the differences between the pre- and post-entrainment PSDs that eventually result in reduced mobilities of the coarse particles (schematic illustration in Fig. 1). Validations of the PSD-based approach using the field data of East Fork River are important because they provide another dimension as to how the new approach performs in real cases.

From the calibration and validation comparisons of the field and laboratory data, the application of the PSD-based approach generally provides adequate predictions of sediment mobility. All the experimental and field data used in this study follow unimodal PSDs. The presented PSD-based approach might simulate biased mobilities for sediments with non-unimodal PSDs. The mobilities of bimodal or trimodal sediments need to be simulated using the detailed sediment mobility simulation approaches such as

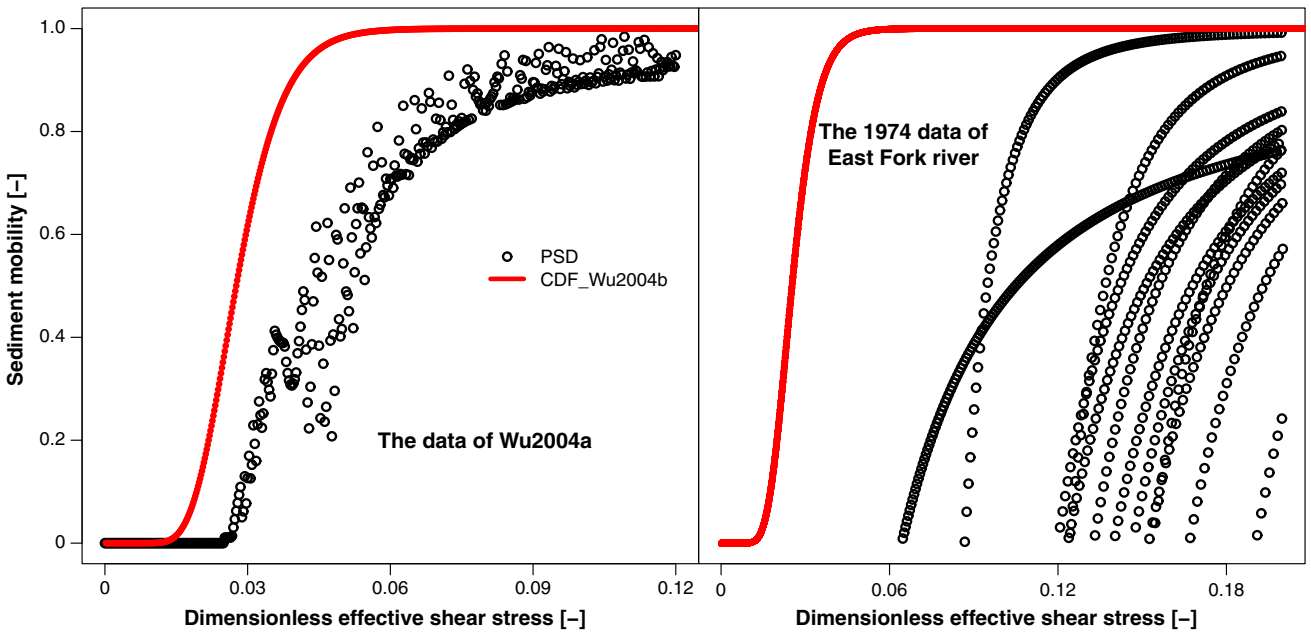

Fig. 2 Size-dependent mobilities estimated with the PSD-based approach using the uniform-sediment-based critical grain size dcr compared to the results predicted with the CDF_Wu2004b

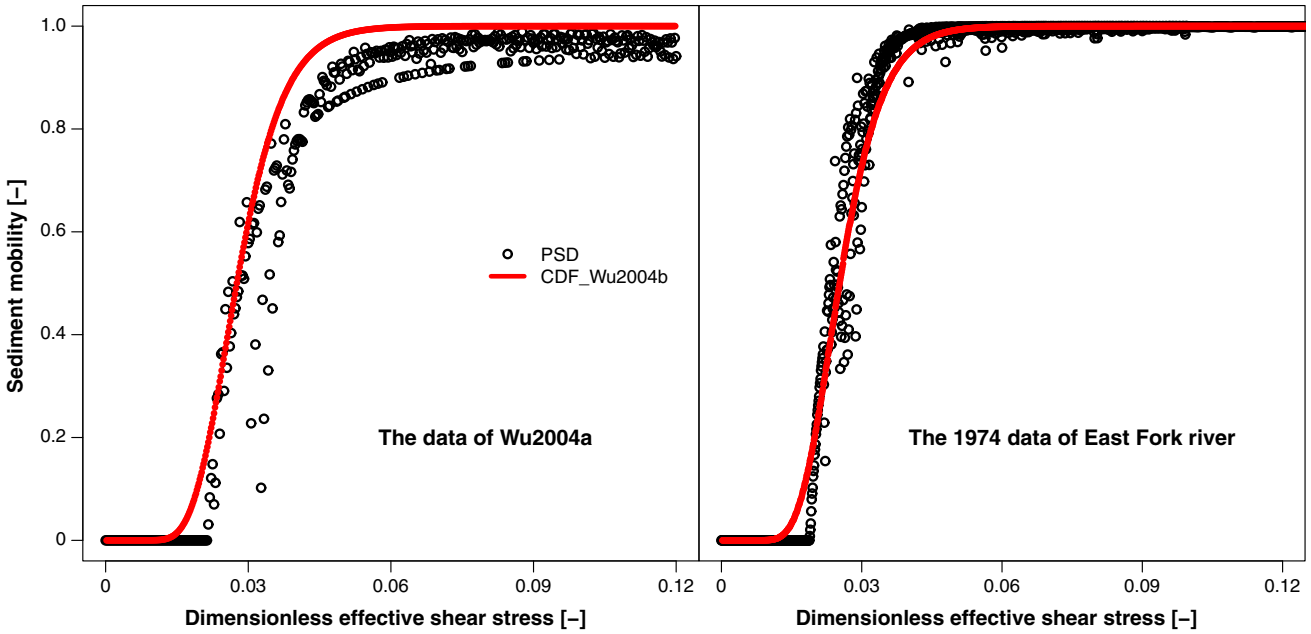

Fig. 3 Size-dependent mobilities estimated with the PSD-based approach using the modified threshold particle size d2 compared to the results predicted with the CDF_Wu2004b

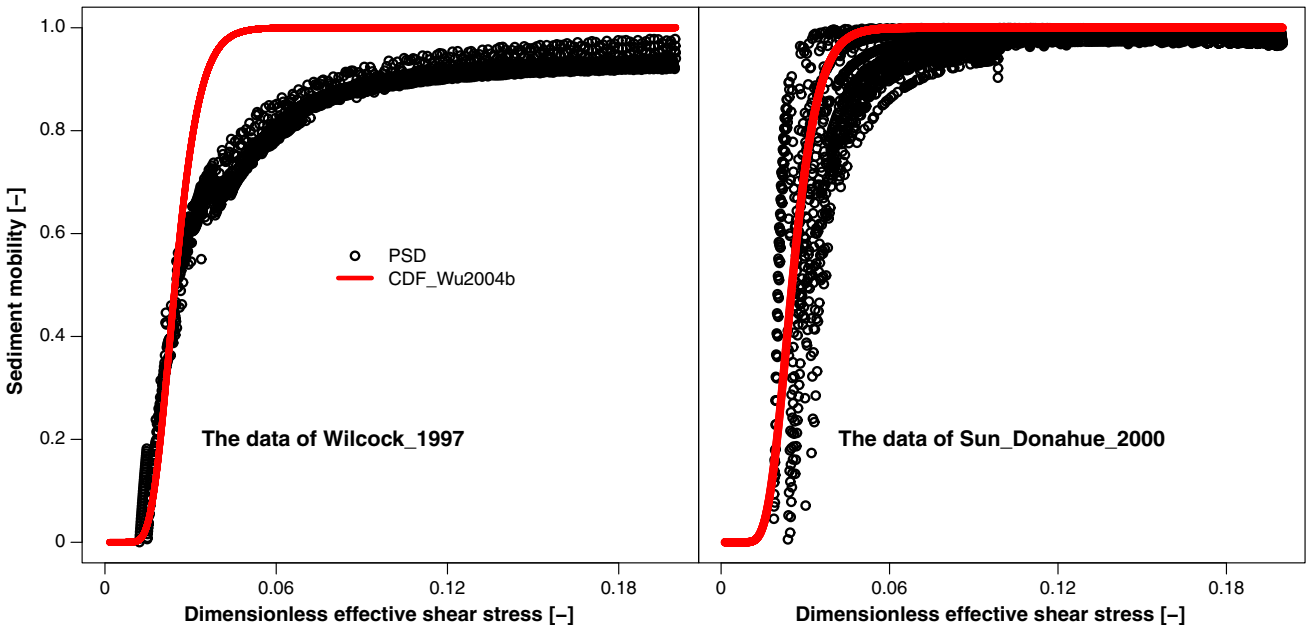

Fig. 4 Size-dependent mobilities estimated with the PSD-based approach for the laboratory datasets of Wilcock and Mcardell (1997) and Sun and Donahue (2000) compared to the results predicted with the CDF_Wu2004b

the method developed by Wu and Yang (2004b). The good news is that many river sediments follow unimodal PSDs and hence their mobilities can be simulated using the PSD-based method. As long as lognormal probability density function (PDF) fits to the particle size distribution (PSD), the new method works whether it is a very fine or a very coarse sediment. However, if a theoretical lognormal PDF doesn't fit to the PSD, it is often the tail part of the distribution that shows a high sensitivity of mobility calculation to the discrepancy. For a coarse sediment sample with a very heavy upper tail (e.g., the bed load data of Leopold and Emmettt (1976) on 05/29/1974), we noticed that the fitted theoretical PDF shows a high discrepancy in the upper tail part. An attempt to have a balanced fit of the theoretical PDF to the PSD eventually led to an underestimated upper tail and an overestimated lower tail. Such a

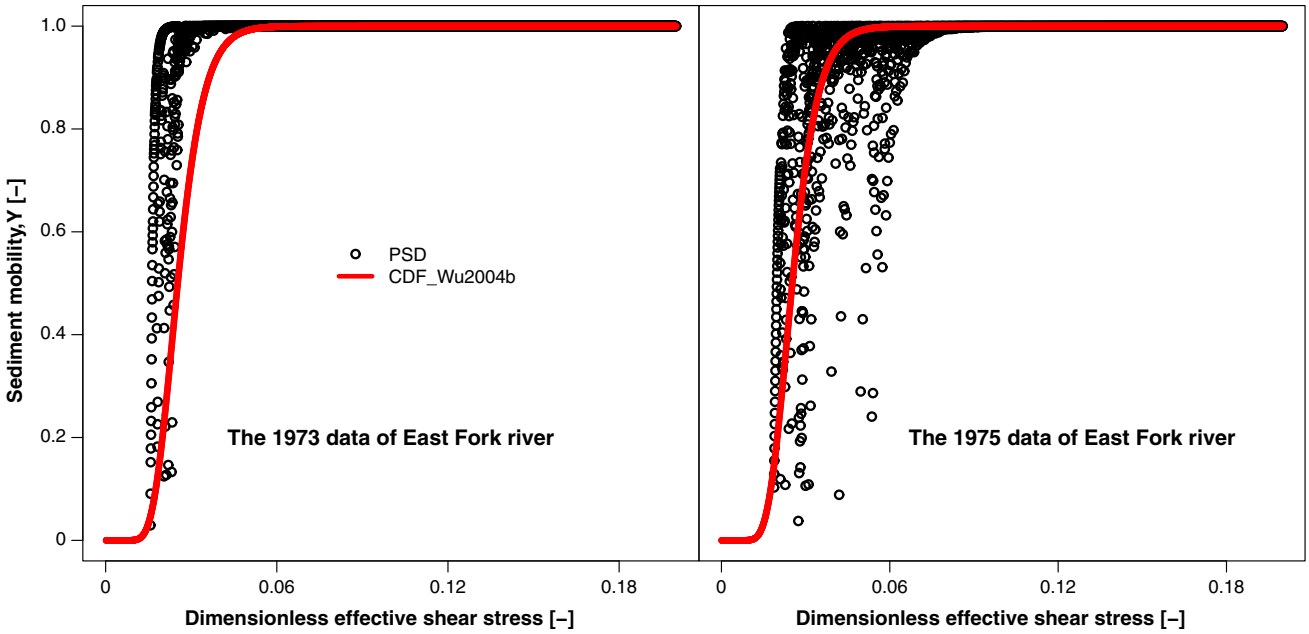

Fig. 5 Size-dependent mobilities estimated with PSD-based approach for the 1973 and 1975 data of East Fork River (Leopold and Emmettt 1976) compared to the results predicted with the CDF_Wu2004b

balanced PDF calibration of coarse sediments with very heavy upper tail might lead to an overestimated mobility of the finer sediments. Based on the empirical bed load data we analyzed from literature, however, this type of PSD are not common. For very fine sediment samples, we expect that the empirical PDF becomes very positively skewed and because lognormal distributions can fit this type of empirical distributions quite well, there will not be no serious problem during mobility calculation.

4 Conclusions

This paper presents a heuristic sediment mobility approach that considers the particle size distribution of mixed-size sediments using probability density functions. The basic assumption underpinning this approach is that the PSDs follow lognormal distributions. The approach estimates the entrained proportion of the bed sediment by calculating the cumulative distribution function corresponding to the sediment finer than the threshold particle size, which is a modified critical particle size of incipient motion. The critical particle size of incipient motion computed for the uniform-size sediment turned out to significantly underestimate the mobility of coarse particles because in mixed-size sediments the coarse particles are subjected to bed shear stresses higher than the average bed shear stress.

Our approach has two novelties. (1) It accounts for the effect of sediment size non-uniformity on the critical particle size of incipient motion, thereby separates the mobile and immobile populations of the mixed-size sediments. (2) It estimates the size-dependent mobilities simply using the pre- and post-entrainment sediment PSDs. The means and standard deviations of the entrained and post-entrainment PSDs are computed using the statistical functions of truncated and mixed size distributions.

Three published laboratory datasets and one field dataset were used to compare the size-dependent mobilities estimated with the PSD-based approach and those predicted with the empirical lognormal CDF approach of Wu and Yang (2004b). The size-dependent mobilities estimated with the PSD-based approach well capture the results predicted with the empirical lognormal CDF approach of Wu and Yang (2004b).

The PSD-based approach represents an important contribution because: (1) it is conceptually heuristic and computationally efficient; (2) it satisfactorily mimics the complex process of sediment entrainment simply using the PSD of bed sediment and the threshold particle size of incipient motion; (3) it can be applied in simple conceptual models that do not need to simulate the detailed hydrodynamics and (4) It can easily be coupled with water quality models to simulate the deposition and resuspension of sediment-bound pollutants.

Appendix 1

See Table 1.

Table 1 Parameters (means and standard deviations) of the best-fit lognormal PSDs

Data source (purpose of use)	Sediment type	Mean of lognormal PSD (mm)	Standard deviation of lognormal PSD (mm)
Wu and Yang (2004b) (calibration)	C1–C7	4.46	3.55
Leopold and Emmettt (1976) (calibration)	5-25-74	0.84	0.79
	5-26-74	0.87	0.90
	5-27-74	1.65	2.16
	5-28-74	2.12	2.78
	5-29-74	7.54	37.34
	5-30-74	2.37	2.50
	5-31-74	2.37	2.50
	6-1-74	1.66	1.52
	6-2-74	2.13	3.26
	6-3-74	1.82	2.39
	6-4-74	1.69	1.95
	6-5-74	1.44	1.48
Wilcock and Mcardell (1997) (validation)	BOMC18	10.43	21.93
	BOMC2	11.04	29.59
	BOMC19	11.94	24.49
	BOMC4	9.44	19.85
	BOMC5	9.44	19.85
Sun and Donahue (2000) (validation)	SS1	0.61	0.53
	SS2	0.75	0.83
	SS3	1.00	1.54
	SS4	1.74	2.67

Appendix 2

See Tables 2, 3, 4 and 5.

Table 2 The data used for calibration from Wilcock and Mcardell (1997)

Run	Depth (m)	Sediment type	Width (m)	Velocity (ms^{-1})	τ_0 (Nm^{-2})	Sand fraction (f_s)
1	0.122	BOMC18	0.6	0.55	2.0	0.34
2	0.112	BOMC2	0.6	0.6	2.5	0.34
3	0.126	BOMC19	0.6	0.66	3.2	0.34
4	0.094	BOMC4	0.6	0.87	5.0	0.34
5	0.088	BOMC5	0.6	1.08	7.3	0.34

Table 3 The data used for validation from Wu and Yang (2004a)

Run	Depth (m)	Sediment type	Width (m)	Velocity (ms^{-1})	τ_0 (Nm^{-2})	Sand fraction (f_s)
1	0.080	C-1	0.4	0.52	2.04	0.30
2	0.090	C-2	0.4	0.55	2.16	0.30
3	0.085	C-3	0.4	0.71	3.76	0.30
4	0.083	C-4	0.4	0.64	3.08	0.30
5	0.085	C-5	0.4	0.78	4.46	0.30
6	0.092	C-6	0.4	0.81	4.75	0.30
7	0.080	C-7	0.4	0.73	4.06	0.30

Table 4 The data used from Sun and Donahue (2000) and the calculated velocity and the bed shear stress corrected for the effect of smooth side walls

Run	Q (l/s)	Depth (m)	Slope ($\times 10^{-3}$)	Sediment type	Width (m)	τ_0 (Nm^{-2})	Sand fraction (f_s)
1	19.54	0.12	0.5	SS1	0.5	0.467693	0.97
2	25.52	0.143	0.5	SS1	0.5	0.535637	0.97
3	14.5	0.084	1	SS1	0.5	0.717914	0.97
4	19.37	0.09	1	SS2	0.5	0.73032	0.93
5	8.02	0.048	1.5	SS2	0.5	0.644144	0.93
6	14.3	0.07	1.5	SS2	0.5	0.909693	0.93
7	19.89	0.082	1.5	SS3	0.5	1.032175	0.85
8	9.49	0.05	2	SS3	0.5	0.899586	0.85
9	23.68	0.091	2	SS4	0.5	1.551264	0.74

Table 5 The data used for validation from Leopold and Emmettt (1976)

No.	Depth (m)	Slope	Velocity (ms^{-1})	τ_0 (Nm^{-2})	Sand fraction (f_s)
1	0.48	0.0007	0.76	3.090	0.59
2	0.74	0.0007	0.92	4.601	0.59
3	1.27	0.0007	1.15	7.416	0.59
4	1.60	0.0007	1.28	8.996	0.59
5	2.01	0.0007	1.41	10.850	0.59
6	1.68	0.0007	1.31	9.408	0.59
7	1.33	0.0007	1.18	7.691	0.59
8	1.38	0.0007	1.20	7.966	0.59
9	1.43	0.0007	1.22	8.240	0.59
10	1.59	0.0007	1.27	8.996	0.59
11	1.52	0.0007	1.25	8.652	0.59
12	1.47	0.0007	1.23	8.378	0.59

References

Abuodha JOZ (2003) Grain size distribution and composition of modern dune and beach sediments, Malindi Bay coast, Kenya. J Afr Earth Sci 36:41–54. https://doi.org/10.1016/S0899-5362(03)00016-2

Agrawal YC, Mikkelsen OA, Pottsmith HC (2012) Grain size distribution and sediment flux structure in a river profile, measured with a LISST-SL instrument. Sequoia Scientific, Inc, Bellevue

Armanini A, Di Silvio G (1988) A one-dimensional model for the transport of a sediment mixture in non-equilibrium conditions. J Hydraul Res 26:275–292. https://doi.org/10.1080/00221688809499212

Biron PM, Robson C, Lapointe MF, Gaskin SJ (2004) Comparing different methods of bed shear stress estimates in simple and complex flow fields. Earth Surf Process Landf 29:1403–1415. https://doi.org/10.1002/esp.1111

Bouchez J, Metivier F, Lupker M et al (2011) Prediction of depth-integrated fluxes of suspended sediment in the Amazon River: particle aggregation as a complicating factor. Hydrol Process 25:778–794. https://doi.org/10.1002/hyp.7868

Buscombe D, Conley DC (2012) Effective shear stress of graded sediments. Water Resour Res 48:1–13. https://doi.org/10.1029/2010WR010341

Church M, Wolcott J, Maizels J (1990) Palaeovelocity: a parsimonious proposal. Earth Surf Process Landf 15:475–480. https://doi.org/10.1002/esp.3290150511

Eisenberg B, Sullivan R (2008) Why is the sum of independent normal random variables normal? Math Mag 81:362–366. https://doi.org/10.2307/27643141

Fowlkes EB (1979) Some methods for studying the mixture of two normal (lognormal) distributions. J Am Stat Assoc 74:561–575. https://doi.org/10.2307/2286973

Graf WH, Song T (1995) Bed-shear stress in non-uniform and unsteady open-channel flows. J Hydraul Res 33:699–704. https://doi.org/10.1080/00221689509498565

Jafari M, Hemmat A, Sadeghi M (2011) Comparison of coefficient of variation with non-uniformity coefficient in evaluation of grain drills. J Agric Sci Technol 13:643–654

Lavelle JW, Mofjeld HO (1987) Do critical stresses for incipient motion and erosion really exist? J Hydraul Eng 113:370–385. https://doi.org/10.1061/(ASCE)0733-9429(1987)113:3(370)

Leopold LB, Emmettt WW (1976) Bedload measurements, East Fork River, Wyoming. Proc Natl Acad Sci USA 73:1000–1004

Lopez F, Garcia MH (2001) Risk of sediment erosion and suspension in turbulent flows. J Hydraul Eng 1:231–235

Oh J, Tsai CW (2017) A stochastic multivariate framework for modeling movement of discrete sediment particles in open

channel flows. Stoch Environ Res Risk Assess. https://doi.org/10.1007/s00477-017-1410-3
Rhodes DG (1995) Newton–Raphson solution for gradually varied flow. J Hydraul Res 33:213–218. https://doi.org/10.1080/00221689509498671
Rilstone P (2002) Econometric analysis of count data. J Am Stat Assoc 97:361–362. https://doi.org/10.1198/jasa.2002.s458
Safik A, Safak M (1994) Moments of the sum of correlated log-normal random variables. In: Vehicular technology conference. IEEE, Stockholm, pp 140–144
Schulte AM, Chaudhry MH (1987) Gradually-varied flows in open-channel networks. J Hydraul Res 25:357–371. https://doi.org/10.1080/00221688709499276
Shrestha NK, Leta OT, De Fraine B et al (2013) OpenMI-based integrated sediment transport modelling of the river Zenne, Belgium. Environ Model Softw 47:193–206. https://doi.org/10.1016/j.envsoft.2013.05.004
Soulsby R, Whitehouse R (1997) Threshold of sediment motion in coastal environments. In: Pacific coasts and ports' 97: proceedings of the 13th Australasian coastal and ocean engineering conference and the 6th Australasian port and harbour conference, vol 1. Centre for Advanced Engineering, University of Canterbury, p 145
Sun Z, Donahue J (2000) Statistically derived bedload formula for any fraction of nonuniform sediment. J Hydraul Eng 126:105–111
Sundborg A (1956) The River Klarälven: a study of fluvial processes author(s): Åke Sundborg Published by: Wiley on behalf of Swedish Society for Anthropology and Geography Stable. http://www.jstor.org/stable/520140. Accessed 14 April 2016. 14: 10 UTC. Geogr Ann 38:125–237
Tayfur G, Singh VP (2007) Kinematic wave model for transient bed profiles in alluvial channels under nonequilibrium conditions. Water Resour Res. https://doi.org/10.1029/2006WR005681
Vanoni VA, Brooks NH (1957) Laboratory studies of the roughness and suspended load of alluvial streams. California Institute of Technology, Pasadena
Wilcock PR, Mcardell BW (1997) Partial transport of a sand/gravel sediment flume. Water Resour Res 33:235–245. https://doi.org/10.1029/96WR02672
Wilcock PR, Southard JB (1988) Experimental study of incipient motion in mixed-size sediment. Water Resour Res 24:1137–1151. https://doi.org/10.1029/WR024i007p01137
Wilcock PR, Southard JB (1989) Bed-load transport of mixed-size sediment: fractional transport rates, bed forms, and the development of a coarse bed-surface layer. Water Resour Res 25:1629–1641
Wu F-C, Wang C-K (1998) Higher-order approximation techniques for estimating stochastic parameter of a sediment transport model. Stoch Hydrol Hydraul 12:359–375. https://doi.org/10.1007/s004770050025
Wu W, Wang SSY (2000) Movable bed roughness in alluvial rivers. J Hydraul Eng 125:1309–1312
Wu F-C, Yang K-H (2004a) A stochastic partial transport model for mixed-size sediment: application to assessment of fractional mobility. Water Resour Res 40:1–18. https://doi.org/10.1029/2003WR002256
Wu F-C, Yang K-H (2004b) Entrainment probablities of mixed-size sediment incorporating near-bed coherent flow structures. J Hydraul Eng 130:1187–1197
Wu W, Wang SAMSY, Jia Y (2000) Nonuniform sediment transport in alluvial rivers Transport de sédiments non uniformes en rivière alluviale. J Hydraul Res 38:427–434. https://doi.org/10.1080/00221680009498296